APPLIED MATERIALS AND TECHNOLOGY

Research Article

Jamt.ejournal.unri.ac.id

Optimization Of Pelleting Parameters For Producing Composite Pellets Using Zeolitic Material From Fly Ash

D. A. Fungaro*, T. C. R. Bertolini

Instituto de Pesquisas Energéticas e Nucleares, IPEN–CNEN/SP, São Paulo, SP, Brazil

ABSTRACT: Zeolitic material in powder form was prepared from fly ash by direct activation treatment. The fly ash-based zeolite was pelletizing using different inorganic (calcium hydroxide, bentonite, kaolinite) and organic (dextrin) binders with varying percentage. The aim of this study was to produce granular zeolitic material for application in wastewater treatment. The zeolitic materials were analyzed by XRF, XRD, SEM, FTIR, TG-DTG and Nitrogen adsorption/desorption isotherm. Compression and impact tests were used to evaluate the deformation and breakage behaviour of spherical granules. The best performance was obtained by zeolite granular containing 5 wt.% bentonite and 5 wt.% kaolinite with mechanical strength and satisfactory water resistance. The synthesis of pelletized zeolite from by-products derived from coal combustion provides not only environmental and economic benefits, but also contributes to achieving the principles of sustainable development.

Key words: fly ash, pelletization, zeolite, mechanical performance

1. INTRODUCTION

Zeolites are the most representative microporous materials composed of alumina and silica tetrahedra with wide applications in catalysis (petrochemical industry, refining processes, fine chemical production) and in gas storage and separation. Also, due to their ability to select molecules by size and shape and ion exchange selectivity, zeolites have been employed in removing heavy metal (Zn^{2+}, Cd^{2+}, Pb^{2+}, Cu^{2+}), radioactive contaminants (Cs^{+}, Sr^{2+}, U^{4+}), dyes (crystal violet, acid orange 8) and others toxic pollutants from wastewater [1, 2].

Materials useful for zeolite synthesis can be silicon-and aluminum-rich chemicals, from industrial waste, agricultural sources, and by-products, recognized as low-cost raw materials. Coal combustion by-products (CCBs) are a cheap and abundant materials, rich in minerals containing silicon and aluminum, making it suitable as a starting material for the synthesis of zeolites and an attractive alternative to disposal. The global annual production is approximately 150 to 200 million tons of bottom ash and between 600 and 800 million tons of fly ash [3, 4].

Various methods for preparing synthetic zeolites are described in literature (Azizi et al., 2021; Ren et al., 2020; Zhang et al., 2022) [1, 3, 5]. One of the most common methods of obtaining zeolites from CCBs is the conventional hydrothermal synthesis, also known as, direct activation method. Brief, the ash is dispersed in a strongly alkaline solution to extract the silica and alumina and submitted to a heat treatment with a temperature in the range of 90–200 °C for a period of up to 24 h. During this period, reactants in the amorphous phase is replaced by the crystalline phases. This method is considered as a simple and cost-effective approach in zeolitization because low resources are consumed. Zeolitic product obtained is a mixture of multiple zeolites and the yield is about 20–60 wt.% [6, 7].

Zeolitic materials based on CCBs are obtained in the form of a fine powder [8-11]. In fixed-bed reactor processes, the effective utilization of zeolite requires that the powder is structured in the form of solid bodies mechanically stable (cylinders, pellets, beads, spheres, etc.).

In order to form granulated zeolite, it is necessary that binder is added to fine powder in the agglomeration techniques. The most commonly used binders are organic compounds (carboxymethylcellulose, starch, dextrin), aluminosilicate clay, (bentonite, attapulgite, kaolinite), synthetic compounds (alumina, silica), or a combination of these materials. The type of binder to be applied depends on the granulation method and the utilization of the granulated zeolite [12, 13]. In most cases, zeolites are agglomerated with 20% of a binder [14-16].

The objective of this work is to evaluate the behavior of different binders to agglomerate zeolitic material synthesized from fly ash using wet granulation. To optimize the properties of granules, different binders in several percentages were used; then, the properties of products were studied.

2. MATERIALS AND METHOD

2.1 Materials

All chemicals used for experimental studies were of analytical grade. Coal fly ash sample was collected in the Thermoelectric Complex Jorge Lacerda, located in the Santa Catarina State, Brazil. Physico-chemical properties of fly ash have been reported in previous studies [17, 18]. Binders were commercially produced material. Sodium hydroxide (97%) and sodium aluminate (100%) obtained from Sigma-

Received : October 26, 2022
Revised : November 29, 2022
Accepted : December 25, 2022

Aldrich Pty. Ltd. (Australia) were used in the preparation of zeolite synthesis.

2.2 Zeolite powder synthesis

Conventionally hydrothermal treatment was used in the zeolite synthesis: 20 g of coal fly ash were mixed with 160 mL of 3.5 mol L^{-1} NaOH aqueous solution in a Teflon vessel (ash/solution ratio = 0.125 g mL^{-1}). This mixture was heated to 100 °C for 24 h. The suspension was filtered through a quantitative filter paper and the solid was repeatedly washed with deionized water until the pH of filtrate is at ~ 11. The solid was dried at 100 °C for 24 h. The zeolitic material obtained was labeled as ZC [11].

2.3 Preparation of zeolite in granular form

ZC was mixed with binder and homogenized. Then, deionized water with ratio dry mixture mass:volume = 1:1 was slowly poured into a cavity in the center of the container containing the dry mixture until a paste was obtained. After homogenization, the pasty mixture was molded into spherical granules. After the molding step, the material was dried in an oven at 100 °C for 2 h and calcined in a muffle at 500 °C for 2 h. The diameters of granules ranged between 3 mm and 6 mm. ZC content was maintained at 90 and 95 wt. %. Eleven pelletized zeolite samples (ZP1 to ZP11) with dextrin, calcium hydroxide, bentonite, kaolinite, and a mixture of the binders with different amounts are listed in Table 1. Figure 1 illustrates one of the pellet samples produced.

Table 1. Composition of binders used in pelleting of zeolite powder

Pelletized Zeolite	Composition (wt.%)			
	Dextrin	Calcium Hydroxide	Bentonite	Kaolinite
ZP1	5	0	0	0
ZP2	10	0	0	0
ZP3	0	10	0	0
ZP4	0	0	0	10
ZP5	0	0	10	0
ZP6	0	5	5	0
ZP7	5	5	0	0
ZP8	0	0	2	8
ZP9	0	0	5	5
ZP10	0	0	8	2
ZP11	0	0	2.5	2.5

2.4 Characterization of materials

Physico-chemical properties of fly ash have been reported in previous studies [17, 18]. The mineralogical compositions were determined by X-ray diffraction analyses (XRD) with Rigaku Miniflex 2 diffractometer with Cu anode using Co Kα radiation at 40 kV and 20 mA over the range (2θ) of 5–80° with a scan time of 0.5°/min. The chemical composition was determined by X-ray fluorescence (XRF) in Rigaku RIX-3000 equipment. Thermal analysis was performed by thermogravimetry on the Mettler-Toledo equipment model TGA/SDTA 851 and each sample (~10 mg) was heated from 25 to 1000 °C at a heating rate of 10 $^{0}C{\cdot}min^{-1}$, under an oxygen flush (50 $mL{\cdot}min^{-1}$). The scanning electron micrographs were performed using a FEI QUANTA FEG 650 microscope. Vibration spectra of the samples were determined by Fourier Transform Infrared Spectroscopy (FTIR) (Perkin Elmer Frontier) within a wavelength from 4000 cm^{-1} to 400 cm^{-1}. Textural properties of the samples were measured from N_2 adsorption/desorption isotherms at 77 K (Micromeritics, TriStar II 3020). The samples were purged with nitrogen gas for 12 h at 150 °C. The specific surface area was calculated by the Brunauer–Emmet–Teller (BET) [19]; the microporous surface area, external surface area, and micropore volume were evaluated by the *t*-plot method [20]; the pore diameter and mesopore volume were obtained by the Barrett–Joyner–Halenda (BJH) method. The pore-size distribution was calculated by analyzing both the adsorption and desorption branches of the isotherm using the Barrett-Joyner-Halenda method [21].

Fig. 1. Pelletized zeolite sample (ZP9)

Cation exchange capacity was determined by a previously described procedure [22]. The stability in water of the granular zeolite was determined by weighing the pellet mass before and after the cation exchange capacity test. Workability was related to the ease of handling and molding the paste consisting of powdered zeolite, binder and water to form pellets (H=high; M= medium; L=low). All tests were done in triplicates.

The drop test consisted of dropping the material from a height of 100 cm onto a metallic surface and recording the number of drops that each granule withstood until disintegrating. The compressive strength test was performed for the samples that were selected in the drop test. A texturometer model TA.XT.PLUS, brand STABLE MICRO SYSTEMS was used. The test was carried out at room temperature, using a 500 N load cell and constant velocity equal to 0.02 mm s^{-1}, until the primary fracture (F_F). The

tests were repeated five times per series of samples. The characteristic fracture strength (σF) was calculated from the ratio of the fracture force (F_F) related to the cross-sectional area (A) of the granule [23]:

$$\sigma_F = \frac{F_F}{A} = \frac{F_F}{\pi R^2} \quad (1)$$

3. RESULTS AND DISCUSSIONS

3.1 Chemical and mineralogical characterization of zeolite powder

The chemical composition of the zeolitic material (ZC) determined by X-ray fluorescence (XFR) is shown in Table 2. The zeolitic product is mainly composed of silica, alumina, calcium oxide, iron oxide and sodium oxide. The presence of sodium is the result of the addition of NaOH solution in the hydrothermal treatment. Elements present in fly ash, such as Fe, Ca, Mg, Ti, Mn, etc. were also found in zelitic material [17]. The cation exchange capacity values obtained for fly ash used as raw material and zeolitic material was 0.083 meq g^{-1} and 1.84 meq g^{-1}, respectively. The CEC value of ZC was 20 times higher than fly ash confirming that zeolitic material has a high potential to be used as cation exchanger.

Table 2. Chemical composition of the major elements of ZC

Oxides	wt. %	Oxides	wt. %
SiO_2	34.7	ZrO_2	0.067
Al_2O_3	23.3	ZnO	0.056
CaO	10.1	P_2O_5	0.052
Fe_2O_3	7.80	MnO	0.052
Na_2O	7.56	SrO	0.036
TiO_2	1.76	Cr_2O_3	0.032
MgO	1.00	CeO_2	0.024
SO_3	0.557	Cl	0.020
K_2O	0.510	others	< 0.016
BaO	0.080	loss of ignition (%)	12.2

The phases in zeolitic material obtanined by X-ray diffraction (Figure 2) were hydroxysodalite (JCPDS 31-1271) and NaX (JCPDS 38-0237) as zeolitic phases with peaks of quartz (JCPDS 85-0796) and mullite (JCPDS 74-4143) of ash that remained after the treatment. The diffractograms also show the presence of halo typical of material amorphous. Hydroxysodalite is always created in the majority phase of zeolite content in the synthetized product obtained by conventional hydrothermal treatment due to its greater stability [6, 8, 9, 24].

3.2 Effect of the type and amount of binder on the characteristics of granular zeolite

In the first phase, pellets with eleven different binder types and percentages were prepared with and without calcination. The choice of the binders was based on procedures reported in the literature [25-28].

Clay-like binders not only improve the mechanical stability, but they also contribute to the physical and chemical properties of the powder being shaped. However, the addition of clays binders with alumina and silica content can significantly alter some zeolite properties, in terms of structure or acidity [12]. Calcium hydroxide is one of the most popular types of inorganic binders and is usually used as a pellet hardening agent. Organic binders might be easily removed from the shaped composites upon thermal treatment, thus not altering the physical and chemical properties of the initial powder. However, they may fail to give sufficient mechanical strength to the pellets.

The primary goal of using binders was to enhance the mechanical stability of the granules. The investigated properties of drop test of non-calcined and calcined zeolitic materials pelletized are presented in Table 3.

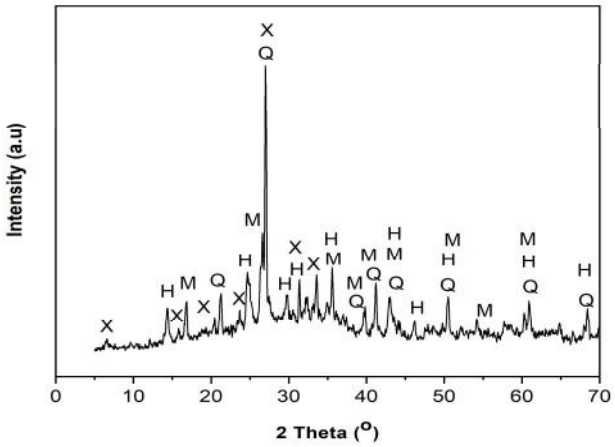

Fig. 2. XRD diffractogram of zeolite in powder form (H = hydroxysodalite; X= NaX; Q = Quartz, M = mullite).

Table 3. Drop test of non-calcined and calcined zeolitic materials

Pelletized Zeolite	Drop test[1]	
	Non-calcined zeolite	Calcined zeolite
ZP1	1	1
ZP2	1	1
ZP3	1	2
ZP4	1	4
ZP5	4	71
ZP6	1	1
ZP7	1	1
ZP8	1	7
ZP9	19	70
ZP10	21	99
ZP11	5	14

(1) number of drops without breaking the pellets

The results varied widely, depending on the type and composition of the binders used. The strength of pelletized zeolite samples before calcination were not satisfactory with the majority breaking in the first fall, indicating that a calcination would be necessary. Combined pelleted samples with bentonite and kaolinite (ZP9 and ZP10) were an exception, because showed a relatively high drop strength value even without calcination.

The reason for the significant increase in the strength of the granules after the calcination process is probably the physical and chemical changes in the binders that occur during the heat treatment [29]. Calcination increased the mechanical stability of the pellets and destroys the surface area and activity of the clay [16]. After the solidification step by calcination, shaped zeolite bodies contain an inter-particular and interconnected pore systems, which is classified as hierarchical [30].

Organic binder (dextrin) and calcium hydroxide were not able to create enough strong bonds with the surfaces of zeolitic material (sample ZP1, ZP2 and ZP3) even after calcination.

The greatest resistances have been reached with the pellet composition containing bentonite alone (ZP5) or mixed with kaolinite in greater or equal percentage (ZP9 and ZP10) and the pellets from the stoichiometric mixture contained 90 wt.% zeolite.

The compactness and the resistance of the granules to the mechanical forces are essential for the use of the granules in various applications; therefore, a measurement of the forces at which granules broke was conducted to evaluate the effectiveness of the binder in the granules. Based on the results, the *mechanical strength* of ZP5, ZP9 and ZP10 samples after calcination *was* measured by force-displacement curves (Figure 3). The average values of mechanical properties are summarized for examined granulates in Table 4.

The force-displacement curves for ZP5, ZP9 and ZP10 samples presented similar behavior (Figure 3). The samples exhibit dominant elastic-plastic properties before primary breakage occurs. Linear-elastic portion of the curve was observed only at the beginning of stressing (< 0.1 mm). After the breakage point, the multiple stressing leads to the failure of the fragments. Similar mechanical behaviour during compression was observed with commercial synthetic zeolitic molecular sieves of the type 4A in the form of granules [23, 31-33].

Table 4. Macroscopic mechanical properties of the granule samples

Sample	Binder (% wt)		Breakage Force (N)	Fracture Strength (Mpa)
	Bentonite	Kaolinite		
ZP5	10	0	49.7	2.6
ZP9	5	5	34.8	1.5
ZP10	8	2	30.9	1.6

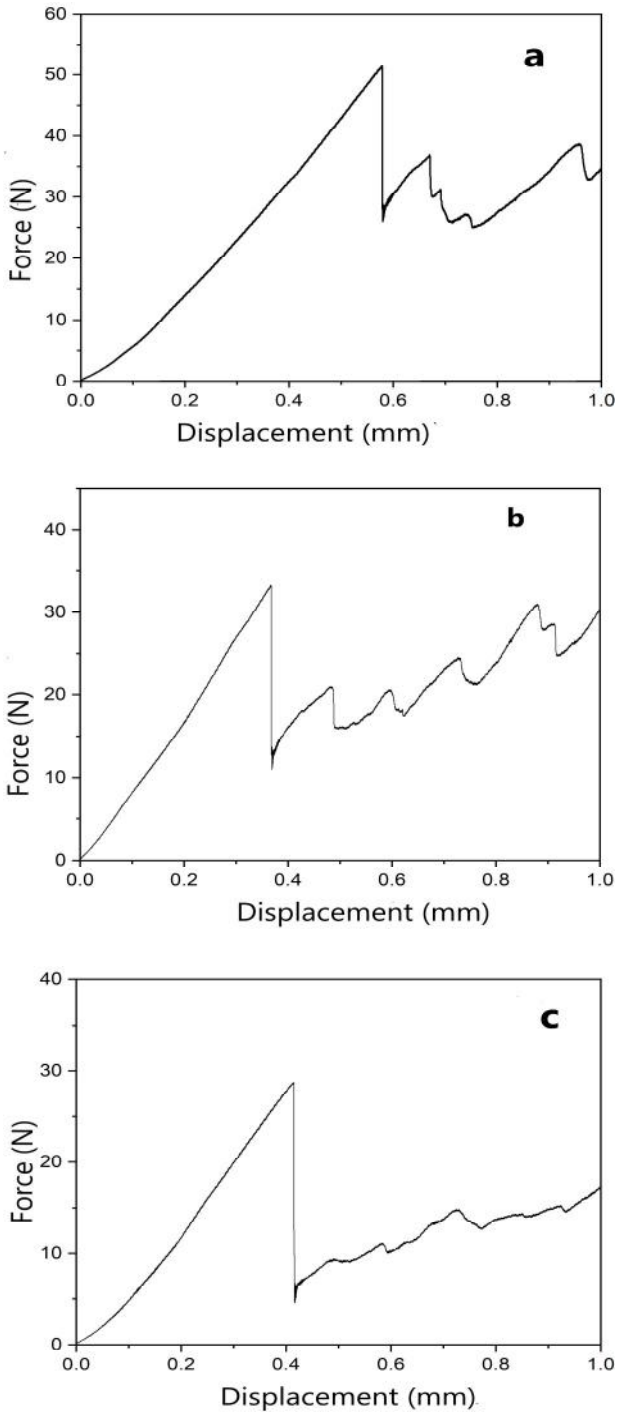

Fig. 3. Force-displacement curve of (a) ZP5; (b) ZP9; (c) ZP10

The increase in bentonite content increases strength due to improvement in interaction between the zeolite and clay particle. The addition of kaolinite into the composition decreased the compressive strength due to increase in pore size and heterogonous distribution of secondary pore system [16, 34]. The breakage force of commercial zeolite (Köstrolith 4AK) prepared with *attapulgite* was 23.8 ± 7.7 N, a lower value than the samples synthesized with residue [31].

The properties including workability, water stability and cation exchange capacity values of granular zeolitic materials are shown in Table 5. The granular zeolite ZP5, despite

Table 5. Characteristics of granular zeolites with different binder

Sample	Binder (% wt)		Workability[1]	Pellet water stability[1]	CEC[2] (meq g^{-1})
	Bentonite	Kaolinite			
ZP5	10	0	M	L	Collapsed
ZP9	5	5	H	H	1.75
ZP10	8	2	H	M	1.70
ZC		-	-	-	1.84

(1) H=high; M= medium; L=low; (2) Cation exchange capacity

having greater mechanical strength than the other samples, showed less stability in water and the structure collapsed. ZP9 and ZP10 samples presented cationic exchange capacity values close to that of powdered zeolite (ZC) and others similar properties (workability and breakage force). However, the greatest stability in water was observed for ZP9.

Table 6. Chemical composition of bentonite and kaolinite

Oxides	Bentonite (wt.%)	Kaolinite (wt.%)
SiO_2	51.4	47.4
Al_2O_3	15.0	34.8
Fe_2O_3	9.82	1.27
MgO	2.24	< 0.001
CaO	1.74	< 0.001
Na_2O	1.42	0.120
TiO_2	1.40	1.15
K_2O	0.579	0.041
Cl	0.180	0.060
V_2O_5	0.042	< 0.001
BaO	0.036	< 0.001
MnO	0.033	< 0.001
P_2O_5	0.032	0.127
Cr_2O_3	0.021	< 0.001
SrO	0.019	0.017
ZnO	0.019	< 0.001
NiO	0.013	0.009
Rb_2O	0.007	< 0.001
Nb_2O_2	0.005	< 0.001
SO_3	< 0.001	0.230
CuO	< 0.001	0.009
PbO	< 0.001	0.019
Ga_2O_3	< 0.001	0.010

Therefore, sample with the mentioned composition of 90 wt.% zeolite with 5 wt.% bentonite and 5 wt.% bentonite (ZP9) was selected as optimum granular zeolitic material to be used as an adsorbent material in the treatment of liquid effluent in a fixed bed column. This obtained material and binders were characterized by different complementary techniques.

3.3 Characterization of binders

The chemical compositions of the bentonite and kaolinite are given in Table 6. From Table 6, it is identified that both clays mainly contained silicon oxide (SiO_2) and aluminum oxide (Al_2O_3), dominant constituents of all clay minerals. The relatively high percentage of Fe_2O_3 (~10%) is typical for most Brazilian bentonites [35]. The Fe_2O_3 and TiO_2 were the main impurities (1.2-1.3%) for kaolinite.

The X-ray patterns of used binders are illustrated in Figure 4. The bentonite (Figure 4a) contains mainly montmorillonite and impurities such as quartz, cristobalite and kaolinite. Kaolinite is the predominant mineral phase, which can be identified by its characteristic XRD peaks at 12.34° and 24.64° 2θ (Figure 4b) [36].

3.4 Granular zeolite characterizations obtained by the optimized method

The chemical composition of the granular zeolitic material ZP9 is reported in Table 7, along with the SiO_2/Al_2O_3 ratio. An increase of silica and alumina in the chemical composition of the zeolite after pelletization compared to powder zeolite (Table 2) was confirmed, since these are the main constituents of binding agents (bentonite and kaolinite) used in the process.

Figure 5 shows the XRD pattern of the as-prepared granular zeolite and powder zeolite. After pelletization, no new diffraction peaks was observed, indicating no new crystalline phase formation, that is important to maintain the zeolite properties. The addition of bentonite and kaolinite as a binder also did not cause a significant change in peaks intensity.

Figure 6a and 6b illustrates the SEM images of zeolitic material ZC at different magnifications. The surface is constituted of rough-surfaced and spheroidal crystals, indicating that zeolite crystals were deposited on the surface of fly ash particles during the hydrothermal treatment. The morphologies of zeolitic material are similar to the typical appearances found in the earlier published SEM observations [37-39].

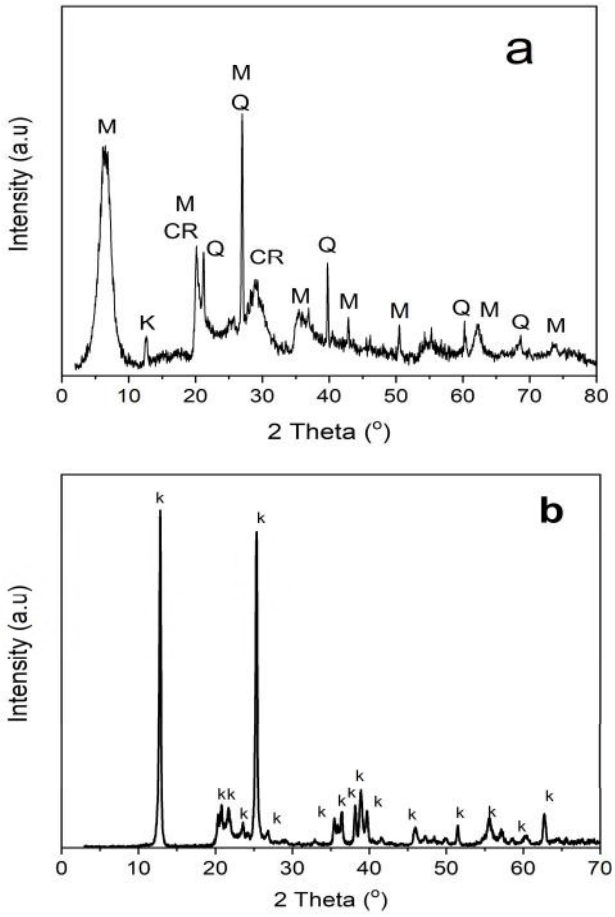

Fig. 4. XRD diffractogram of (a) bentonite (M: montmorillonite, Q: quartz, k: kaolinite, CR: cristobalite); (b) kaolinite (k: kaolinite)

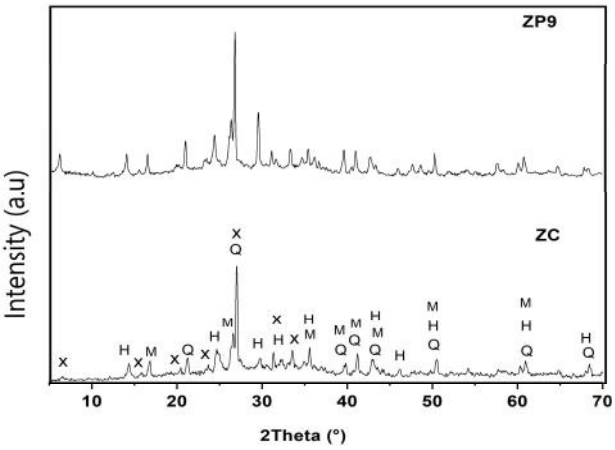

Fig. 5. XRD diffractogram of power zeolite and granular zeolite (H = hydroxysodalite; X= NaX; Q = Quartz, M = mullite)

The agglomerated ball-like morphology is commonly associated with hydroxysodalite zeolite [40]. It is evident that the morphological representation of hydroxysodalite and mixture with others zeolite types through SEM data does not always allow the particular phase identity [41].

In the micrographs obtained from granular zeolite is observed that the zeolite particles are surrounded by the binders bentonite and kaolinite (Figure 6c and 6d).

Table 7. Chemical composition of the major elements of ZP9

Oxides	wt. %	Oxides	wt. %
SiO_2	46.7	K_2O	0.487
Al_2O_3	26.6	MnO	0.048
CaO	8.66	SO_3	0.474
Na_2O	7.40	P_2O_5	0.045
Fe_2O_3	6.41	ZnO	0.043
TiO_2	1.46	SrO	0.031
MgO	1.37	Cr_2O_3	0.025
BaO	0.069	Cl	0.020
ZrO_2	0.068	Y_2O_3	0.014
CeO_2	0.057	SiO_2/Al_2O_3	1.80

The main functional groups characteristics of the granular and powder zeolites were identified by FTIR (Figure 7). FTIR analysis of the samples revealed the preservation of the structure of zeolite in form of powder after the pelletization process. The bands at 459-466 cm^{-1} were ascribed to the internal vibration of T-O (T= Si, Al) bending [42]. The vibrations observed at 560 cm^{-1} are corresponding to a super-position of symmetrical stretching vibrations of the Si-O-Si and the bending vibrations corresponding to O- Si –O [43]. The bands at 662-667 cm^{-1} and 728-729 cm^{-1} were attributed to symmetry stretching vibration of O-Si-O and the band at 695 cm^{-1} was attributed to symmetry stretching vibration Al-O-Si [37]. Vibrations reflected at 995–1009 cm^{-1} are assigned to the asymmetric stretching vibrations characteristic of T-O-T bridge bonds in TO_4 tetrahedra belonging to aluminosilicates with sodalite structure [44, 45]. The bands in the regions of 1453-1472 cm^{-1} and at about 876 cm^{-1} were assigned to the C−O stretching [37, 46]. The band observed at 1638-1645 cm^{-1} correspond to the H-OH deformation and are usually evidence of the presence of hydrated compounds whose water is strongly linked to the molecular structure of the compound [47]. The bands at 3438-3446 cm^{-1} are characteristic of OH hydrogen bonded to the oxygen ions of the zeolite framework [5, 48].

The profile of the thermogravimetric curves of ZC and ZP9 are shown in Figure 8. From Figure 8a, the great loss of mass weight associated with loss of free and physically adsorbed water inside the zeolite pores occurred between 33.8 °C and 49.0 °C (7.24%). It can be seen that sample showed continuous weight loss until 400 °C due dehydration, after that it became almost constant. In the second stage, the mass loss between 296.68 °C and 716.03 °C (6.26%) can be attributed to the decomposition of $CaCO_3$ from fly ash used as raw material for the zeolite synthesis [49]. The profile of the thermogravimetric curves of the granular zeolite (Fig. 8b) was maintained in relation to that obtained for the powdered zeolite, thus confirming the thermal stability of the material after the pelletization process.

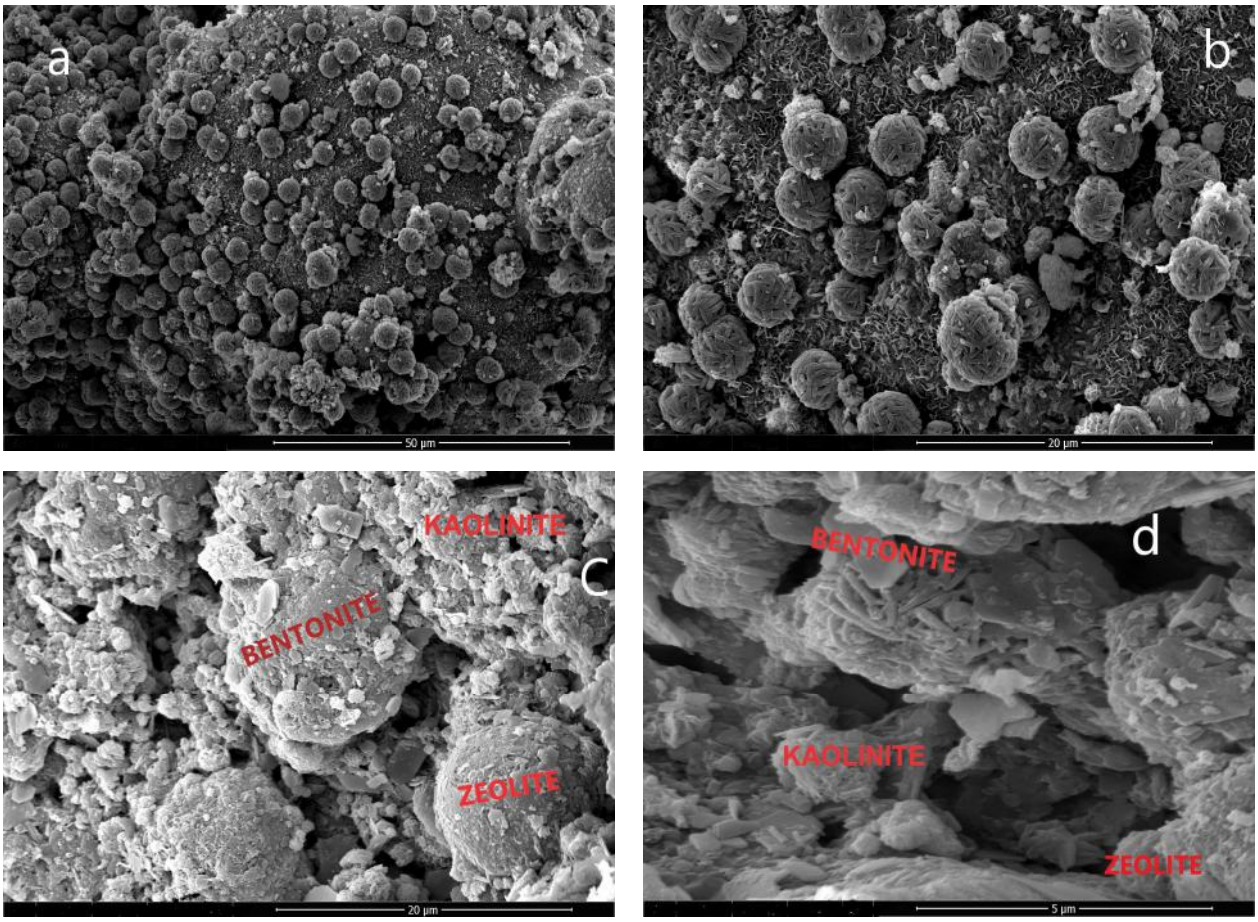

Fig. 6. SEM micrograph of zeolites with different magnifications (a) ZC- 10000 x; (b) ZC- 40000 x; (c) ZP9- 10000 x; (d) ZP9 - 40000 x

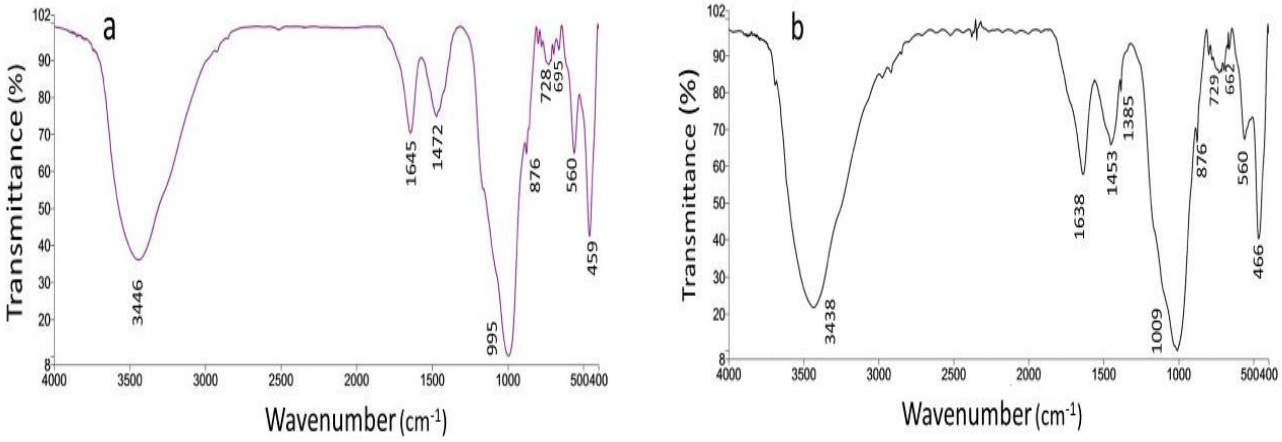

Fig. 7. FTIR spectra of the as-synthesized zeolitic material (a) ZC powder; (b) ZP9 pelletized

The N_2 adsorption-desorption isotherm of the zeolitic material in powder form is presented in Figure 9a, while the pore size distribution curve determined by the Barret-Joyner -Hatenda (BJH) model is presented in Figure 9b. The isotherm for the sample was of type IV and exhibited a well-defined H3 hysteresis loop according to the IUPAC classification, relative to the mesoporous structure [50]. A bimodal pore distribution was observed due to the presence of mainly mesopores centered around 50 Å and 250 Å (Figure 9b).

The granular zeolitic material shows mesoporosity characteristics as it is evident in the adsorption/desorption isotherm, similar to the adsorption/desorption isotherm of zeolite powder (Figure 10a). The pore sizes of the sample were concentrated in the 30-680 Å range (Figure 10b). However, the pore diameter distribution shows a unimodal distribution with a peak around 250 Å. Probably, the presence of bentonite and kaolinite as binders in the structure of the granules resulted in the blocking of pores of smaller diameter [51].

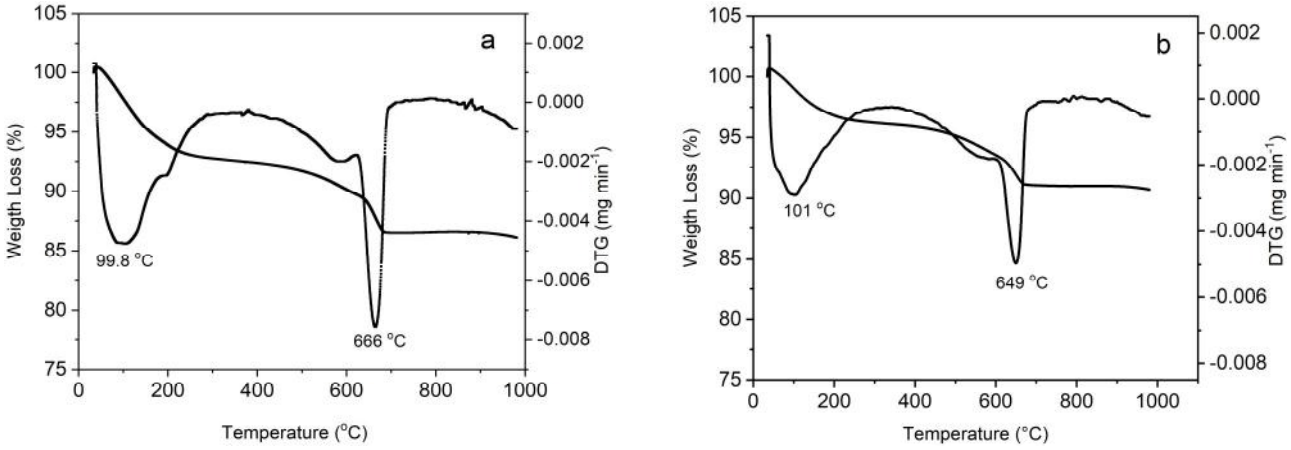

Fig. 8. TG and DTG curves of (a) ZC; (b) ZP9

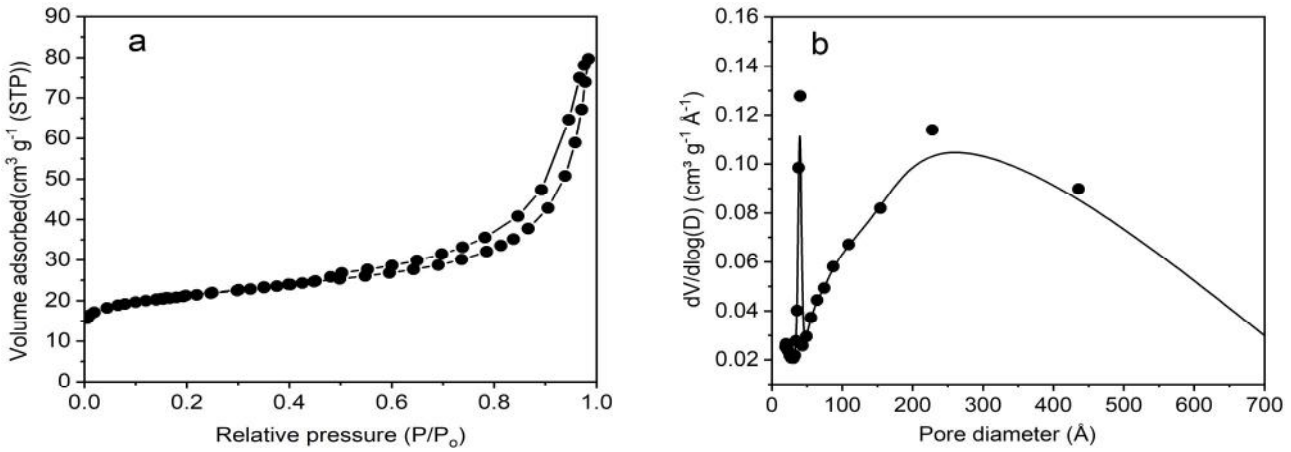

Fig. 9. (a) Nitrogen adsorption-desorption isotherms; (b) Pore diameter distribution curve for ZC

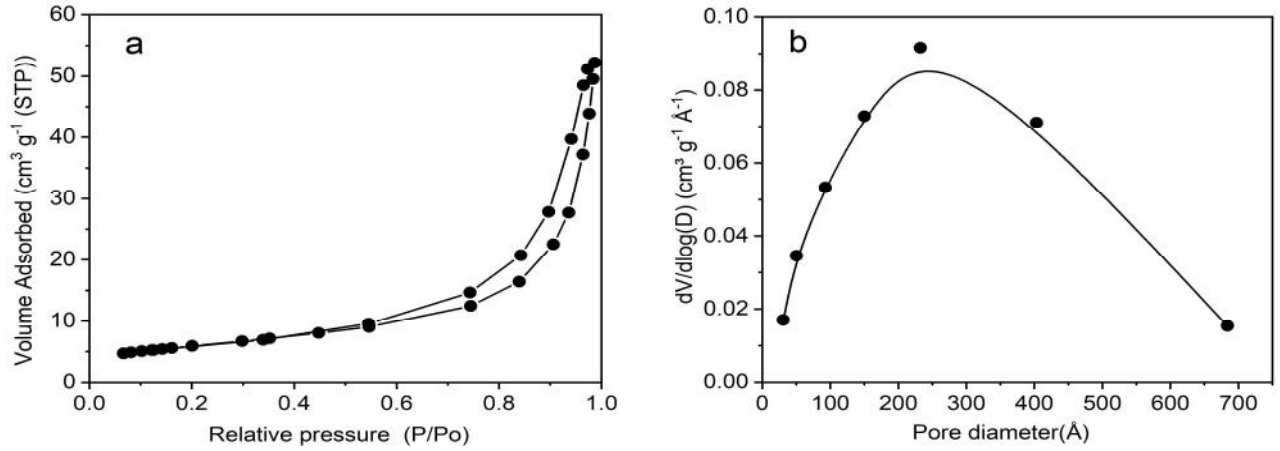

Fig. 10. (a) Nitrogen adsorption-desorption isotherms; (b) Pore diameter distribution curve for ZP9

Table 8. Textural properties of zeolitic materials

SAMPLE	S^1_{BET} ($m^2 g^{-1}$)	S^2_{Micro} ($m^2 g^{-1}$)	S^3_{exter} ($m^2 g^{-1}$)	V^4_{Micro} ($cm^3 g^{-1}$)	D^5_{poro} (Å)	V^6_{Meso} ($cm^3 g^{-1}$)
ZC	76.57	38.52	38.05	0.01633	108.8	0.1110
ZP9	21.20	2.104	19.11	0.000775	125.3	0.08129

[1]BET specific surface area; [2-4] microporous surface area, external surface area, micropore volume; [5-6] poro diameter, mesopore volume

The BET, t-plot and BJH methods were employed to calculate the textural properties of synthesized zeolites before (ZC) and after (ZP9) the addition of bentonite and kaolinite to the conformation of the sample into spherical shape (Table 8). As shown in Table 8, the values of surface area and micropore volume of zeolitic powder are higher than pelletized zeolitic material, as indicated in the pore diameter distribution curve due to presence of binders.

4. CONCLUSIONS

In this study, fly ash was activated by conventional hydrothermal treatment. Zeolite phases, such as, Na-X and hydroxysodalite were identified in zeolitic material in powdered form. Inorganic and organic binders were used to shape the zeolite powder into spherical granules using wet granulation process. The pellets were characterized in terms of physico-chemical, mechanical properties, and adsorption capacity. The best condition for the spherical adsorbent can be obtained for the sample prepared using 90 wt.% zeolitic material, 5 wt.% bentonite and 5 wt.% kaolinite. Although the pelletization decreased the textural properties, the granular zeolitic material exhibited similar characteristics to the zeolitic material powder, mainly in relation to the cation exchange capacity. The results show the possibility for using the readily available, low-cost waste (CCBs) to produce granular zeolitic material, following the concept of turning waste into value-added material for environmental applications related to Sustainable Development Goal 12 (target 12.5).

AUTHOR INFORMATION

Corresponding Author
*Email: dfungaro@ipen.br

ORCID
D. A. Fungaro : 0000-0003-1618-0264

ACKNOWLEDGMENTS

The authors are grateful to Conselho Nacional de Desenvolvimento Científico e Tecnológico (CNPq), Coordenação de Aperfeiçoamento de Pessoal de Nível Superior (CAPES) for supporting this study and Jorge Lacerda coal-fired power plant for providing coal ash sample.

REFERENCES

[1] Azizi, D., Ibsaine, F., Dionne, J., Pasquier, L-C., Coudert, L., Blais J-F. 2021. "Microporous and macroporous materials state-of-the-art of the technologies in zeolitization of aluminosilicate bearing residues from mining and metallurgical industries: A comprehensive review." Microporous Mesoporous Mater., 318, 111029.

[2] Khaleque, M. M., Alam, M. M., Hoque, M., Mondal, S., Haider, J. B., Xu, B., Johir, M. A. H., Karmakar, A. K., Zhou, J. L., Ahmed, M. B., Moni, M. A. 2020. "Zeolite synthesis from low-cost materials and environmental applications: A review." Environ. Adv., 2, 100019.

[3] Zhang, X-Y., Li, C-Q., Zheng S-L., Di, Y-H., Sun, Z-M. 2022. "A review of the synthesis and application of zeolites from coal-based solid wastes." Int. J. Miner. Metall. 29, 1-21.

[4] Yoldi, M., Fuentes-Ordoñez, E. G., Korili, S. A., Gil, A. 2019. "Zeolite synthesis from industrial wastes." Microporous Mesoporous Mater., 287, 183-191.

[5] Ren, X., Qu, R., Liu, S., Zhao, H., Wu, W., Song, H., Zheng, C., Wu, X. Gao, X. 2020. "Synthesis of Zeolites from Coal Fly Ash for Removal of Harmful Gaseous Pollutants: A Review." *Aerosol Air Qual. Res.,* 20, 1121-1144.

[6] Längauer, D., ˇCablík, V., Hredzák, S., Zubrik, A., Matik, M., Danková, Z. 2021. "Preparation of synthetic zeolites from coal fly ash by hydrothermal synthesis." Materials., 14, 1267-1292.

[7] Harja, M. and Ciobanu, G., 2020. Eco-friendly nano-adsorbents for pollutant removal from wastewaters, in Kharissova, O., Martínez, L., Kharisov, B. (eds), Handbook of Nanomaterials and Nanocomposites for Energy and Environmental Applications. Switzerland: Springer Nature.

[8] Bertolini, T. C. R., Alcântara, R. R., Izidoro, J. C., Fungaro, D. A. 2015. "Adsorption of Acid Orange 8 dye from aqueous solution onto unmodified and modified zeolites." Orbital: Electron. J., 7, 358-368.

[9] Bertolini, T. C. R., Izidoro, J. C., Alcântara, R. R., Grosche, L. C., Fungaro, D. A. 2015. "Surfactant-modified zeolites from coal fly and bottom ashes as adsorbents for removal of crystal Violet from aqueous solution." Acta Velit, 1, 78-94.

[10] Bertolini, T. C. R., Izidoro, J. C., Magdalena, C. P., Fungaro, D. A. 2013. "Adsorption of crystal violet dye from aqueous solution onto zeolites from coal fly and bottom ashes." Orbital: Electron. J., 5, 179-191.

[11] Izidoro, J. C., Fungaro, D. A., Santos, F. S., Wang, S. 2012. "Characteristics of Brazilian coal fly ashes and their synthesized zeolites." Fuel Process. Technol." 97, 38-44.

[12] Bingre, R., Louis, B., Nguyen, P. 2018. "An overview on zeolite shaping technology and solutions to overcome diffusion limitations." Catalysts, 8, 163-181.

[13] Gleichmann, K., Unger, B., Brandt, A. 2016. Industrial Zeolite Molecular Sieves, in Belviso, C., (ed), Zeolites, Rijeka, Croatia: IntechOpen.

[14] Ainun, S. B., Kugaann, R., Chow, M. F. 2018. "Phosphorus and nitrogen treatment of reservoir water using zeolite." Int. J. Eng. Technol., 7, 333-337.

[15] Ciosek, A. L. and Luk, G. K. 2014. "A feasibility study of a clay-zeolite media as a removal technology of total phosphorus from wastewater." Int. J. Environ. Pollut., 2, 96-102.

[16] Jasra, R. V., Tyagi, B., Badheka, Y. M., Choudary, V. N., Bhat, T. S. G. 2003. "Effect of clay binder on sorption and catalytic properties of zeolite pellets." Ind. Eng. Chem. Res., 42, 3263-3272.

[17] Bertolini, T. C. R. 2019. Synthesis and characterization of zeolitic material granular of coal ash and evaluation in the application as adsorbent. Thesis Doctorate,

Instituto de Pesquisas Energéticas e Nucleares, São Paulo, SP, Brazil. (in Portuguese).

[18] Bertolini, T. C. R., Guilhen, S. N., Fungaro, D. A. 2017. Pellets Manufactured from Coal Fly Ash: Preparation, Characterization and Environmental Applications, in Parker, J. (ed.). Fly Ash: Properties, Analysis and Performance. Hauppauge: Nova Science Publisher.

[19] Brunauer, S., Emmett, P. H., Teller, E. 1938. "Adsorption of gases in multimolecular layers." J. Am. Chem. Soc., 60, 309-319.

[20] Harkins, W. D. and Jura, G. 1944. "Surfaces of solids. XIII. A vapor adsorption method for the determination of the area of a solid without the assumption of a molecular area, and the areas occupied by nitrogen and other molecules on the surface of a solid." J. Am. Chem. Soc., 66, 1366-1373.

[21] Barrett, E. P., Joyner, L. G., Halenda, P. P. 1951. "The determination of pore volume and area distributions in porous substances. I. computations from nitrogen isotherms." J. Am. Chem. Soc., 73, 373-380.

[22] Izidoro J. C., Fungaro D. A., Abbott J. E., Wang, S. 2013. "Synthesis of zeolites X and A from fly ashes for cadmium and zinc removal from aqueous solutions in single and binary ion systems." Fuel, 103, 827-834.

[23] Müller, P., Antonyuk, S., Tomas, J. 2011. "Influence of moisture content on the compression behavior of granules." Chem. Eng. Sci., 34, 1543-1550.

[24] Franus, W., Wdowin, M., Franus, M. 2014. "Synthesis and characterization of zeolites prepared from industrial fly ash." Environ. Monit. Assess., 186, 5721-5729.

[25] Widiastuti, N., Martak, F., Fansuri, H., Ratnasari, M. 2012. "Adsorption of Cu (II) ion on zeolite A synthesized from coal bottom ash in fixed bed column system." 14th Asia Pacific Confederation of Chemical Engineering Congress.

[26] Alaica, A. L. 2012. On-site total phosphorus removal from wastewater, Master of Applied Science, Civil Engineering, Ryerson University, Toronto, Ontario, Canada.

[27] Lee, K., Jo, Y. 2010. "Synthesis of zeolite from waste fly ash for adsorption of CO_2." J. Mater. Cycles Waste Manag., 12, 212-219.

[28] Lee, K. K. 2008. *The use of low-cost zeolites for the removal of selected contaminants and combination with biological process for wastewater treatment.* Thesis Doctorate, University Teknologi Malaysia, Faculty of Science.

[29] Fakin, T., Ristić, A., Horvat, A., Kaučič, V. 2013. Water adsorption study on the zeolite LTA granules, in 5th Serbian-Croatian-Slovenian Symposium on Zeolites, Serbian-Croatian-Slovenian, 56-59.

[30] Mehlhorn, D., Inayat, A., Schwieger, W., Valiullin, R., Karger, J. 2014. "Probing mass transfer in mesoporous faujasite-type zeolite nanosheet assemblies." Chemphyschem., 15, 1681-1686.

[31] Müller, P., Russell, A., Tomas, J. 2015. "Influence of binder and moisture content on the strength of zeolite 4A granules." Chem. Eng. Sci., 126, 204–215.

[32] Russell, A., Schmelzer, J., Müller, P., Krüger, M., Tomas, J. 2015. "Mechanical properties and failure probability of compact agglomerates." Powder Technol.", 286, 546-556.

[33] Antonyuk, S., Tomas, J., Heinrich, S., Mörl, L. 2005. "Breakage behaviour of spherical granulates by compression." Chem. Eng. Sci., 60, 4031-4044.

[34] Salem, A. and Sene, R. A. 2011. "Removal of lead from solution by combination of natural zeolite-kaolin-bentonite as a new low-cost adsorbent." Chem. Eng. J., 174, 619-628.

[35] Porras, D. E. V., Angélica, R. S., Paz, S. P. A. 2021. "Practical mineralogical quantification of bentonites supported for a PXRD calibrated hkl model." Braz. J. Geol., 51, e20200088.

[36] Gonçalves, M.V.B., Cardoso, A.V., Parreira, F.V. 2020. "Intercalation experiments for morphological alteration of kaolinite present in iron ore tailings." Cerâmica, 66, 93-105.

[37] Makgabutlane, B., Nthunya, L. N., Musyoka, N., Dladla, B. S., Nxumalo, E. N., Mhlanga, S. D. 2020. "Microwave-assisted synthesis of coal fly ash-based zeolites for removal of ammonium from urine." RSC Adv.,10, 2416-2427.

[38] Shabani, J. M., Babajide, O., Oyekola, O., Petrik, L. 2019. "Synthesis of Hydroxy Sodalite from Coal Fly Ash for Biodiesel Production from Waste-Derived Maggot Oil." Catalysts, 9, 1052-1066.

[39] Shoumkova, A., Stoyanova, V. 2013."Zeolites formation by hydrothermal alkali activation of coal fly ash from thermal power station "maritsa 3'', Bulgaria." Fuel, 103, 533-541.

[40] Makgaba, C. P., Daramola, M. O. 2015. Transesterification of waste cooking oil to biodiesel over calcined hydroxy sodalite (HS) catalyst: a preliminary investigation. Proceedings of the 2015 International Conference on Sustainable Energy and Environmental Engineering. Bangkok, Thailand.

[41] Nanganoa, L. T., Mbadcam, K. J., Kang, S. 2016. "Synthesis of hydroxy-sodalite from fine fractions of sandy clay loam soil (natural aluminosilicate)." Int. J. Chem. Tech. Res., 9, 725-732.

[42] Flanigen, E. M., Khatami, H., Szymanski, H. A. 1971. Infrared structural studies of zeolite frameworks, in Flanigen E.M., and Sand L.B. (eds), Molecular Sieve Zeolites, Advances in Chemistry 101. Washington DC: American Chemical Society.

[43] Jacas-Rodríguez, A., Rodríguez-Pascual, P., Franco-Manzano, D., Contreras, L., Polop, C., Rodriguez, M. A. 2020. "Mixed matrix membranes prepared from polysulfone and Linde Type A zeolite." Sci. Eng. Compos. Mater., 27, 236-244.

[44] Mozgawa, W., Jastrzębski, W., Handke, M. 2005. "Vibrational spectra of D4R and D6R structural units." J. Mol. Struct., 744-747, 663-670.

[45] Szostak, R. 1992. Handbook of Molecular Sieves. New York:Van Nostrand Reinhold.

[46] Kristova, P., Hopkinson, L., Rutt, K. J. 2015. "The effect of the particle size on the fundamental vibrations of the $[CO_3^{2-}]$ anion in calcite." J. Phys. Chem. A., 119, 4891-4897.

[47] Fernández-Jiménez, A., Palomo, A., Vasquez, T., Vallepu, R., Terai, T., Ikeda, K. 2008. "Alkaline activation of blends of metakaolin and calcium aluminate cement. Part I: Strength and microstructural development." J. Am. Ceram. Soc., 91, 1231-1236.
[48] Zhang, G. X., Tang, D., Jiang, G. 2013. "Synthesis of zeolite NaA at room temperature: The effect of synthesis parameters on crystal size and its size distribution," Adv. Powder Technol., 24, 689-696.
[49] Majchrzak-kucęba, I., and Nowak, W. 2004. "Thermal analysis of fly ash-based zeolites." J. Therm. Anal. Calorim., 77, 125-131.
[50] Thommes, M., Kaneko, K., Neimark, A. V., Olivier, J. P., Rodriguez-Reinoso, F., Rouquerol, J., Kenneth, S. 2015. "Physisorption of gases, with special reference to the evaluation of surface area and pore size distribution (IUPAC Technical Report)." Pure Appl. Chem., 87,1051-1069.
[51] Amir, C., Mohammad, K., Javad, A. S., Sareh, A. L. 2011. "Effect of bentonite binder on adsorption and cation exchange properties of Granulated Nano NaY Zeolite." Adv. Mater. Res; 335-336, 423-428.